Diffusion Bonding of TiC or TiB Reinforced Ti-6Al-4V Matrix Composites to Conventional Ti-6Al-4V Alloy

Sergey V. Prikhodko [a*], Dmytro G. Savvakin [b], Pavlo E. Markovsky [b], Olexander O. Stasuk [b], James Penney [a], Amir A. Shirzadi [c & d], Peter D. Davies [e], Helen M. Davies [e]

[a] Department of Materials Science and Engineering, University of California Los Angeles, Los Angeles, CA 90095, USA;

[b] G.V. Kurdyumov Institute for Metal Physics, National Academy of Science of Ukraine, 36, Vernadsky Blvd., 03142, Kiev, Ukraine;

[c] School of Engineering and Innovation, The Open University, Milton Keynes, MK7 6AA, UK;

[d] Department of Materials Science and Metallurgy, University of Cambridge, Cambridge, CB3 0FS, UK;

[e] Institute of Structural Materials, Swansea University Bay Campus, Crymlyn Burrows, Fabian Way, Swansea, SA1 8EN, UK

*corresponding author tel.: +1 (310) 825-9735; email: sergey@seas.ucla.edu

Diffusion Bonding of TiC or TiB Reinforced Ti-6Al-4V Matrix Composites to Conventional Ti-6Al-4V Alloy

The Diffusion Bonding of conventional alloy Ti-6Al-4V (Ti-64) and composites of this alloy with 10% of TiC or TiB fabricated using blended elemental powder metallurgy was successfully carried out at 850 to 1000 °C, with a holding time of 60 minutes under 0.7-1.5 MPa pressure. The metallographic and electron backscattered diffraction studies, as well as the bending and microhardness tests across the bonds are presented as the evidence of joint integrity. The selected experimental parameters do not cause undesirable structural changes (degradation) in the base metals adjacent to the bond interface. Particle reinforcement at ~10% did not appear to modify bonding parameters when compared to the unreinforced Ti-64 alloy.

Keywords: diffusion bonding; titanium alloy; metal matrix composite; TiC; TiB; blended elemental powder metallurgy;

Introduction

Multi-layered structures have recently become very popular since they demonstrate a far advanced set of characteristics that combine different mechanical properties often non-compatible in a single layer structure [1]. Powder metallurgy (PM) is proven to be well-established cost-efficient way for the fabrication of layered structures made of Ti and its alloys, which is simply not possible using traditional cast and wrought technology. Nevertheless, it is not always flawless. Sintering of compacts consisting of layers of heterogeneous composition can lead to cracking, bending, delamination of individual layers and other types of shape alteration due to differences in shrinkage of the different layer materials [2]. Residual porosity in PM products of Ti is another possible problem, which in some cases can adversely affect the mechanical properties and performance of

the structural components. Post-sintering, hot rolling or pressing are some customary ways of reducing the porosity of Ti-based materials to an acceptable level, even near zero if it is needed [3]. It was shown, however, that hot rolling could not be successfully used on multi-layered structures due to the disparity in the plastic flows of different layers [4]. Separate processing of individual layers to their best performance and post processing bonding of the mating subcomponents is a credible pathway for fabrication of the layered materials with highly optimized properties of each individual layer.

Over the past few decades Diffusion Bonding (DB) has become one of the well-recognized joining techniques in metalworking, which is especially suited to the fabrication of complex Ti–6Al–4V (Ti-64) structures [5]. DB is a solid-state and near-net-shape joining process that is carried out well below the melting temperature of the materials being bonded [6, 7]. The applied pressure is sufficient to assure intimate interfacial contact but does not allow the macroscopic deformation of the parts [7]. The deformation is normally confined primarily to surface asperities [8]. It also can be used to joint parts made of different titanium alloys [9] or dissimilar alloying systems [10, 11]. Final mechanical properties of the joint are determined by the microstructure of the bond interface, presence of defects, and microstructural changes that may occur in the base metals adjacent to the bond interface. The mechanisms controlling diffusion bonding have been extensively studied and the optimization of the key parameters that govern the quality of the joint, namely temperature, time and pressure, have been reported [12].

One of the major predicaments when bonding dissimilar alloys is optimization of the bond parameters for two materials with very different physical and mechanical properties. Additionally, some complications can arise due to presence of second phase, possible contaminants such as oxides, etc. [13] and bond defects [9]. The diffusion

bonding of conventional Ti-64 alloy to a Ti-64 based composite has not been reported before and formed the main motivation of the current research. The presence of very hard and brittle reinforcement particles in one of the mating subcomponents, makes the bonded materials dissimilar. The focus of this investigation was on the evolution of interfacial microstructure and reliability of the joints.

Materials and Methods

Samples preparation

In this study DB was performed between the parts made of the alloy Ti-64 and two different types of Ti- 64 based metal matrix composites. The first type of composite contained TiC while the second one contained TiB; both having 10% (vol.) of reinforcement particles. Selected reinforcement particle types are commonly used in titanium alloys composites since they are capable of increasing a structure's moduli without compromising its low specific weight The bonding trials were performed using two different set-ups, labelled in this study as Methods A and B. Cylinder samples Ø10×12 mm were used in Method A and bars 65×10×10 mm were utilized in B. Bars were further machined to an octagonal prism geometry approximately 59×9.2mm (the last is the diameter of the circumscribed circle of the base) to facilitate their clamping, before the bonding.

Samples used for DB were fabricated using blended elemental powder metallurgy (BEPM). Hydrogenated titanium (TiH_2) powder (3.5 % H, wt.) was used as the base powder for fabrication. The TiH_2 powder particles size was < 100 μm. For Ti-64 alloy samples powder of hydrogenated titanium was blended with 60%Al-40%V master alloy powder (particles size < 63 μm). To fabricate the metal matrix composite (MMC) samples, TiB or TiC in powder form were added to the blends and mixed before the pressing. Size of TiC and TiB_2 powders were 1-30 μm and 5-30 μm,

respectively. The powder of TiB_2 expected to chemically transform during the sintering following the in-situ reaction: $TiB_2+Ti=2TiB$. Blends for each sample were added to the die before the pressing. Preform were pressed at 650 MPa using the die-pressing protocol. Sintering of preforms was carried out in vacuum furnace at 1250 °C, for 4h followed by the slow furnace cooling. Such processing provides dehydrogenation of titanium and formation of typical for Ti-64 alloy α-β lamellar structure with the grain size below 100 μm. More details on samples fabrication and specifics of initial microstructure are discussed elsewhere [2]. Sintered bulk samples were used for subsequent diffusion bonding process.

Diffusion bonding: Method A

Cylindrical samples of both composites and conventional Ti-64 alloy were joined using the diffusion bonder operating a 2-kW induction heating system. The bonding process was carried out in vacuum of about 5×10^{-5} mbar. The joining faces of all samples were ground with 1200 grit emery papers and rinsed in acetone just before loading in the diffusion bonder. Temperature of each sample was monitored and controlled with a K-type thermocouple spot-welded on one of the blocks, close to the joint. The bonding temperature was between 850 to 900 °C when applying minimum 1 MPa bonding pressure. The dwell time at the peak temperature was 60 min for all samples. Two samples: one with TiB and another one with TiC composite were bond using identical conditions in Method A, labelled TiB-A and TiC-A correspondingly.

Diffusion bonding: Method B

To facilitate bonding in arrangement B the two specimens (the alloy and MMC) were ground to a finish of 0.4 μm as part of the machining to form the final bonding samples. No extra grinding was performed immediately before bonding. Then the specimens were assembled in to the load train of a servo hydraulic frame via threaded collets. Both

faying surfaces were brought into contact and held under a holding force of 0.02 kN. Bonding was performed in an argon atmosphere to shield the bond region from the local environment. A water-cooled induction coil was placed around both specimens so that the coil's hot zone aligned with the bond region. The bond region was heated to a temperature of 1000 ˚C (+/- 5 ˚C) at a heating rate of approximately 5 ˚C sec and held for 60 minutes at a stress of 0.7 MPa for regime #1, and 1.5 MPa for regime #2. On completion, bonded specimens were air cooled to room temperature. Temperature control was facilitated by N-type thermocouples welded to the surface of the TiB/TiC

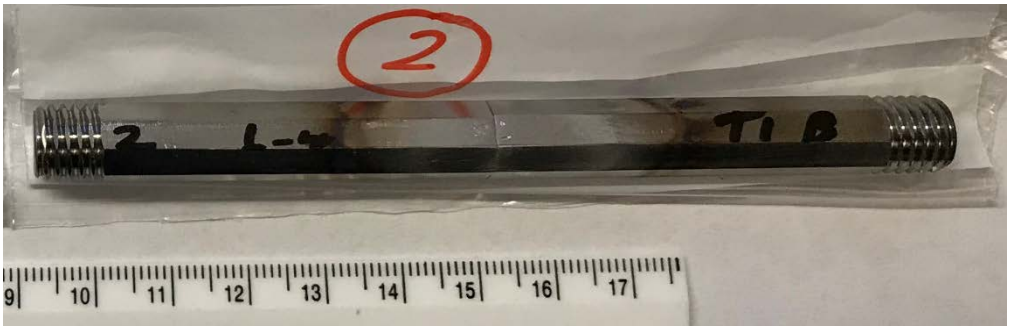

Figure 1. Sample TiB-B2 after DB. The area of the joint is in the middle of the rod. Slight oxidation is observed at about 15 mm distance on both sides from the interface between bond samples

specimens within 1mm of the faying surface. In total, four samples: two with TiB and two other with TiC composite were bond using conditions #1 and #2 in Method B, labelled TiB-B1, TiB-B2, TiC-B1 and TiC-B2. A typical sample after DB is shown in the Figure 1. The major difference between used Methods A and B was the closeness to β-transus temperature of the alloy Ti-64 that is around 995 °C ± 20 °C, which provided a different completion of the $\alpha \rightarrow \beta$ phase transformation. [14] The details of Method A and B can be found in references [15] and [16] correspondingly.

Structure characterization

Light optical microscopy (LOM) in this study was performed using M600 system (Nikon), IX70 (Olympus) and digital optical microscope VHX-1000 (Keyence). SEM study was conducted using variable pressure field emission gun SEM Nova 230

(ThermoFisher) equipped with EDS Noran 7 (ThermoFisher) and tungsten gun high vacuum SEM VEGA3 (Tescan). SEM study in secondary and backscattered electron modes were performed at 10-15 kV. EBSD-EDS study was conducted on the AZtec (Oxford Instruments) system coupled with the SEM LEO 1550VP (Zeiss) operated at 20 kV. Porosity of the samples was measured using the images taken of the polished samples. A number of ~1 mm thick slices were cut from the bonded samples and subjected to bending forces across the bond-lines (transverse) to assess the bond strength qualitatively. Different bending setups were used to maximize the bending force on the bond-line. Microhardness measurements were carried out using MicroMet® 2103 microhardness tester (Buehler Ltd.) with a pyramid diamond tip. Two sets of measurements were taken at loads 0.981 N across the bond interface near the center of the sample as well as at the edge.

Results and Discussion

LOM and low magnification SEM images revealed formation of sound joints in all samples bonded in 1 hour (Fig.2). Some defects were observed close to the edges of the samples which are rather common in diffusion bonding. Such defects are caused by lack of full contact around the edges as a result of manual surface grinding prior to the

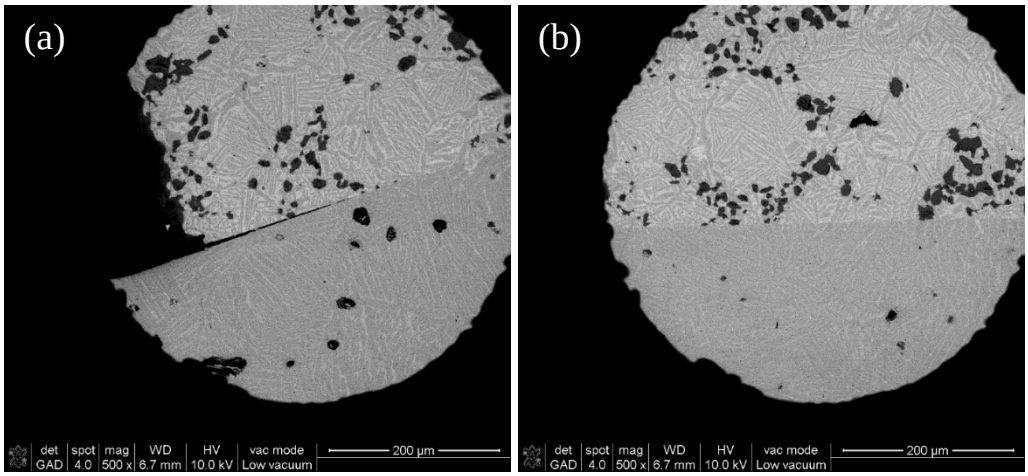

Figure 2. Image of the sample TiC-A demonstrate some of macro defects of the bonding at about 100-150 µm close to the edge of the sample (a), whereas rest of the sample reveal consistency and no visible defects of the bonding alone the interface (b).

bonding. Such a defect was not observed in joints bonded via Method B in which the mating components surfaces were ground as part of the specimens' preparation.

Higher magnification images demonstrate that almost defect-free interfaces were formed between all mating pairs at all processing parameters (Fig.3 and Fig.4). The interface clearly visible at relatively lower magnification images (Fig.3 (a) and Fig.4 (a, c)) becomes practically unrecognizable at higher magnification (Fig.3 (b) and Fig.4 (b, d)).

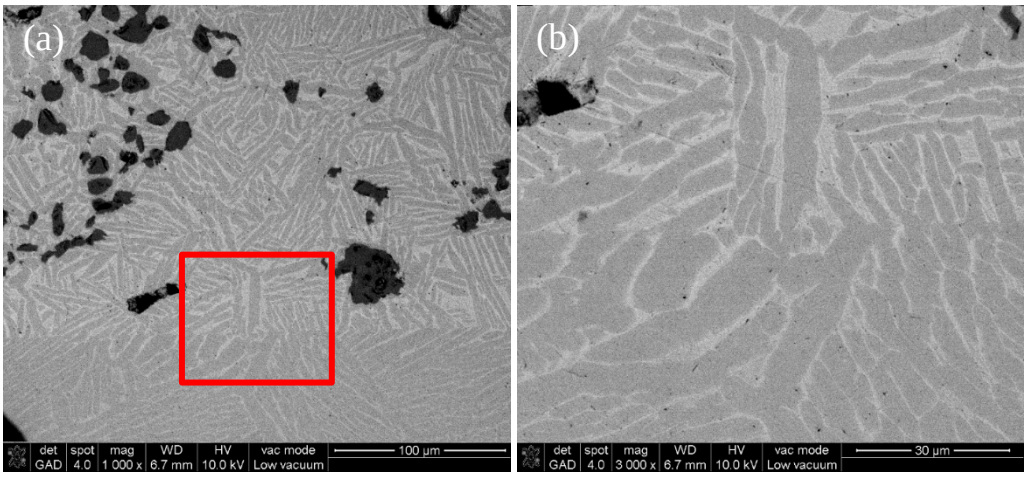

Figure 3. SEM images of the interface resulted on DB of the TiC-A sample processed at bonding temperature between 850 to 900 °C and 1 MPa bonding pressure. The area boxed in (a) is shown in (b).

It is evident that the interface is not completely flat, but displays a wavy surface, which is the result of diffusion taking place between the bonded surfaces, causing their structures intergrowth. The waviness is more pronounced on the samples processed by Method B, which used a higher bonding temperature. At the lower bonding temperature and pressure (850 to 900 °C; 1 MPa) the interface corrugation is about 1-2 µm and it becomes about 4-5 µm when bonded at a higher temperature and slightly higher pressure (1000 °C; 1.5MPa). The shape and orientation of the α-Ti lamellar structure, in the vicinity of interface are similar to the structure in the bulk. Images also show that incorporation of the reinforcement particles within the matrix stay intact after the bonding, as seen in Fig.3 and Fig.4. This observation is true regardless of the particles'

morphology: globular in case of TiC and needles and lamellar in case of TiB particles. When a reinforcement inclusion is located right on the interface it just prevents the structure intergrowth as seen in Fig.4 (d). Any structural defects, such as pores, in the vicinity of the reinforcement particles also remained unchanged. There were no structural differences observed between the samples fabricated using Mode B in regimes #1 and #2

As it was pointed out earlier [17] on DB of Ti-64 alloy, bonding thermal cycles can modify the original Ti-64 lamellar microstructure, transforming the banded structure into an equiaxed structure, due to isothermal annealing below β-transus

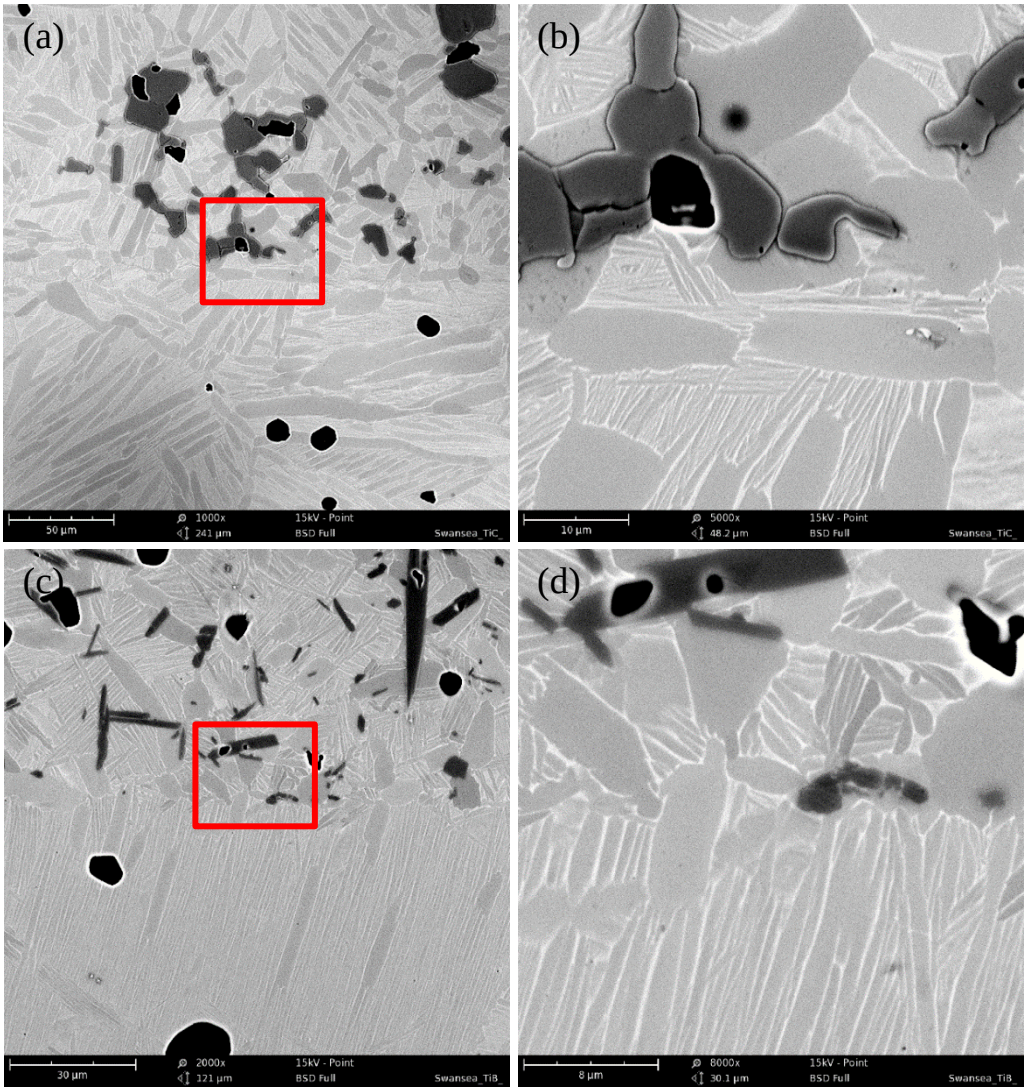

Figure 4. Images of the bond area of the TiC-B2 (a, b) and TiB-B2 (c, d) processed at 1000 °C for 60 minutes at a stress of 1.5MPa. Images (b) and (d) shows boxed areas in (a) and (c) correspondingly.

temperature. This can create a negative effect on mechanical properties. The EBSD orientation maps confirmed the occurrence of cross bond line growth without major plastic deformation of the alloys in vicinity of the interface (Fig.5). In addition, no extensive grain growth or recrystallization was observed close to the bond area. The results of hardness tests measurements within 500 µm across the interface showed hardly any variation in microhardness (Fig.6). Outcomes of the bending tests reveal that due to the very low ductility of the composite, all samples failed within it and about few millimetres away from the joint.

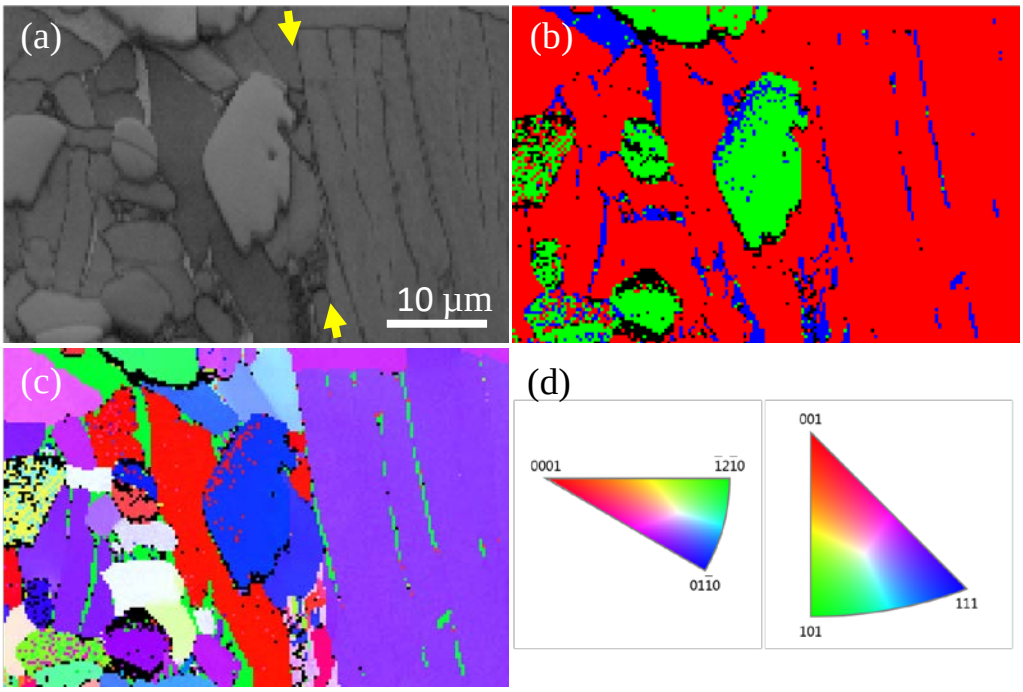

Figure 5. SEM/EBSD results of the DB zone area of TiC-A sample (850 to 900 °C; 1 MPa): band contrast image (a), phase color image (b) and orientation map (c) with stereographic triangles (d) for hexagonal, α-Ti (on the left) and cubic, β-Ti (right) structures. The color is coding different phases in (b): red is for α-Ti, blue is for β-Ti and the green is for TiC. Some defects (noise) of the phase and crystallinity identification are results of not completely removed surface stress on hard TiC inclusions during the sample polishing. Interface between two bonded layers is highlighted with yellow arrows in image A. The α-Ti lamellas are characterized with not deformed structure within the interface. All images are shown at the same magnification.

It is generally accepted [17] that diffusion bonding can be regarded as a process in which the interfacial defects (voids) between two faying surfaces tend to collapse as a result of the diffusion mechanisms which are accelerated by temperature, pressure and time. Elevated pressures favour void collapsing on joints, but tend to produce

undesirable macroscopic deformation and affect the cost. Longer bonding times promote interdiffusion but cause grain growth. In both used methods in this study, A and B, no grain size changes were observed within the area of the DB, compared to initial structure. Most likely, in both cases, the temperature was within the two-phase region, and the pores and reinforcement particles facilitated the lack of grain boundaries mobility. Intragrain structure is also restored on the remnants of the primary α-plates during cooling from DB temperature, which was rather slow since no fine secondary α-phase was observed. The partial healing of pores due to heating + applied pressure could possibly take place, however it was not obvious. Generally, the selected

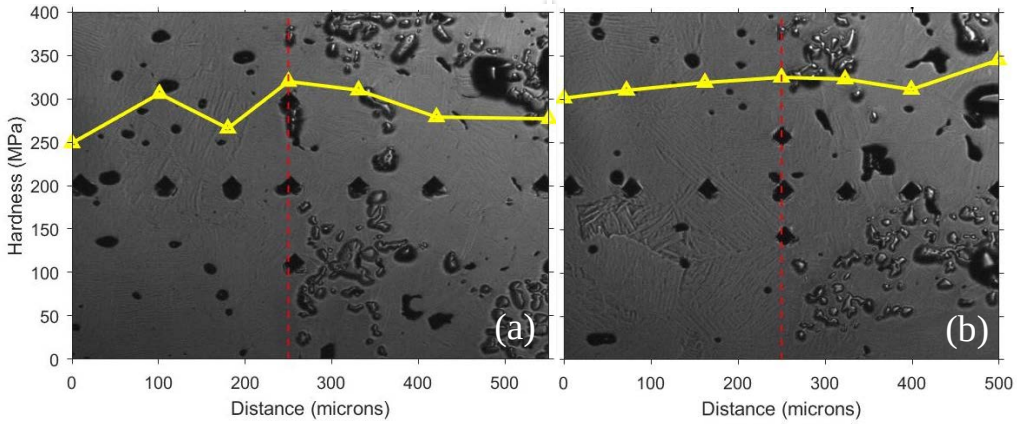

Figure 6. Microhardness test data measured across the bond area of the sample TiC-A (850-900 °C; 1 MPa) superimposed and scaled with the LOM images of the bond showing the diamond pyramid imprints after the test. The data show results measured at the edge of the sample (a) and in its center (b). The interface is shown with dotted red line. The values measured right on the interface are average of three measurements.

experimental parameters do not cause undesirable structural changes (degradation) in the base metal adjacent to the bond interface. Since we do not observe possible negative consequences of tested procession on the structure it appears that an effective compromise between temperature, time and pressure was established in this work leading to consistent quality joints between the Ti-64 alloy and Ti-64 based MMCs. It is worth mentioning that the DB parameters used in this study (in Method A and B) are common for bonding parts made of Ti-64 alloy. Particle reinforcement at ~10% did not appear to alter bonding when compared to the Ti-64 alloy. So, we can conclude that the

MMCs with 10% of reinforcement particles has a similar bond-ability to the conventional Ti-64 alloy. However, previous work has shown that the presence of higher amounts of reinforcement particles, e.g. 30-40%, can significantly compromise the bond integrity and its strength [18].

Conclusions

1. DB was successfully used to join parts made of Ti-64 alloy and Ti-64 MMCs with reinforcement particles (10% vol.) of TiB and TiC. Metallographic and EBSD studies, as well as the bending and microhardness tests across the bonds are presented as the evidence of joint integrity and the lack of microstructure alteration in the vicinity of the joint.

2. The DB of T-64 and Ti-64 with10% TiC or TiB was successfully carried out at 900 to 1000 °C, with a holding time of 60 minutes under 0.7-1.5 MPa pressure. The bonding cycle did not cause any major change in the grain size and the microhardness of the both materials.

3. Particle reinforcement at ~10% did not appear to alter bonding when compared to the unreinforced Ti-64 alloy.

Acknowledgements

The following authors SVP, DGS, PEM, OOS, JP acknowledge funding from the NATO Agency Science for Peace and Security (#G5030).

References

[1] Markovsky PE, Savvakin DG, Ivasishin OM, et al. Mechanical Behaviour of Titanium-Based Layered Structures Fabricated Using Blended Elemental Powder Metallurgy. J Mater Eng Perform. 2019;28(9):5772-5792.

[2] Ivasishin OM, Markovsky PE, Savvakin DG, et al. Multi-Layered Structures of Ti-6Al-4V Alloy and TiC and TiB Composites on Its Base Fabricated Using Blended Elemental Powder Metallurgy. J Mater Proces Tech. 2019;269:172–181.

[3] El-Soudani SM, Yu KO, Crist EM, et al. Optimization of blended-elemental powder based titanium alloy extrusions for aerospace applications. Metall Mater Trans. 2013:A44. DOI 10.1007/s11661-012-1437-5

[4] Prikhodko SV, Markovsky PE, Savvakin DG, et al. Thermo-mechanical treatment of titanium based layered structures fabricated by blended elemental powder metallurgy. Mater Sci Forum. 2018;941:1384-1390.

[5] Bache MR, Tuppen SJ, Voice WE, et al. Novel low cost procedure for fabrication of diffusion bonds in Ti 6/4. Mater Sci Tech. 2009;25(1):39-49.

[6] Rajakumar S, Balasubramanian V. Diffusion bonding of titanium and AA 7075 aluminium alloy dissimilar joints—process modelling and optimization using desirability approach. Int J Adv Manuffacturing Tech. 2016;86:1095–1112.

[7] Ghosh SK, Chatterjee S. On the Direct Diffusion Bonding of Titanium Alloy to Stainless Steel. Mater Manufacturing Proc. 2010;25:1317–1323.

[8] Dunford DV, Wisbey A. Diffusion Bonding of Advanced Aerospace Metallic. Mat Res Soc Symp Proc 1993:314:39-50.

[9] Tuppen SJ, Bache MR, Voice WE. A fatigue assessment of dissimilar titanium alloy diffusion bonds. Int J Fatigue. 2005;27:651–658.

[10] Elrefaey A, Tillmann W. Solid state diffusion bonding of titanium to steel using a copper base alloy as interlayer. J Mater Proc Tech. 2009; 209:2746–2752.

[11] Mo DF, Song TF, Fang YJ, et al. A Review on Diffusion Bonding between Titanium Alloys and Stainless Steels. Advances in Materials Science and Engineering. 2018;15. https://DOI.org/10.1155/2018/8701890

[12] Nicholas MG. Joining processes – introduction to brazing and diffusion bonding. London, Kluwer Academic Publishers; 1998.

[13] Ashworth MA, Jacobs MH, Davies S. Basic mechanisms and interface reactions in HIP diffusion bonding. MaterDesign. 2000;21:351-358.

[14] Pederson R. Microstructure and Phase Transformation of Ti–6Al–4V. Licentiate Thesis, Lulea University of Technology; 2002.

[15] Shirzadi AA, Kocak M, Wallach ER. Joining stainless steel metal foams. Sci Tech Welding Joining. 2004;9(3):277-279.

[16] Davies P, Johal A, Davies H. et al. Powder interlayer bonding of titanium alloys: Ti-6Al-2Sn-4Zr-6Mo and Ti-6Al-4V. Int J Adv Manuf Tech. 2019;103:441–452.

[17] Carrión JG. A Study of Low Temperature Diffusion Bonding Processing ofTI-6AL-4V Alloy for Reducing Costs in SPF/DB Structures. RTO-MP-069 (II), Cost Effective Application of Titanium Alloys in Military Platforms, Loen, Norway, 7-11 May 2001.

[18] Shirzadi AA, Wallach ER. New approaches for the TLP diffusion bonding of aluminium metal matrix composites. Mater Sci Tech. 1997;13(2):135-142.

Figure Captions

Figure 1. Sample TiB-B2 after DB. The area of the joint is in the middle of the rod. Slight oxidation is observed at about 15 mm distance on both sides from the interface between bond samples.

Figure 2. Image of the sample TiC-A demonstrate some of macro defects of the bonding extended inside the sample on about 100-150 μm from the edge (a), whereas rest of the sample reveal consistency and no visible defects of the bonding alone the interface (b).

Figure 3. SEM images of the interface resulted on DB of the TiC-A sample processed at bonding temperature between 850 to 900 °C and 1 MPa bonding pressure. The area boxed in (a) is shown in (b).

Figure 4. Images of the bond area of the TiC-B2 (a, b) and TiB-B2 (c, d) processed at 1000 °C for 60 minutes at a stress of 1.5MPa. Images (b) and (d) shows boxed areas in (a) and (c) correspondingly.

Figure 5. SEM/EBSD results of the DB zone area of TiC-A sample (850 to 900 °C; 1 MPa): band contrast image (a), phase color image (b) and orientation map (c) with stereographic triangles (d) for hexagonal, α-Ti (on the left) and cubic, β-Ti (right) structures. The color is coding different phases in (b): red is for α-Ti, blue is for β-Ti and the green is for TiC. Some defects (noise) of the phase and crystallinity identification are results of not completely removed surface stress on hard TiC inclusions during the sample polishing. Interface between two bonded layers is highlighted with yellow arrows in image (a). The α-Ti lamellas are characterized with not deformed structure within the interface. All images are shown at the same magnification.

Figure 6. Microhardness test data measured across the bond area of the sample TiC-A (850- 900 °C; 1 MPa) superimposed and scaled with the LOM images of the bond showing the diamond pyramid imprints after the test. The data show results measured at the edge of the sample (a) and in its center (b). The interface is shown with dotted red line. The values measured right on the interface are average of three measurements.